

# EvidMTL: Evidential Multi-Task Learning for Uncertainty-Aware Semantic Surface Mapping from Monocular RGB Images

Rohit Menon

Nils Dengler

Sicong Pan

Gokul Krishna Chenchani

Maren Bennewitz

**Abstract**—For scene understanding in unstructured environments, an accurate and uncertainty-aware metric-semantic mapping is required to enable informed action selection by autonomous systems. Existing mapping methods often suffer from overconfident semantic predictions, and sparse and noisy depth sensing, leading to inconsistent map representations. In this paper, we therefore introduce EvidMTL, a multi-task learning framework that uses evidential heads for depth estimation and semantic segmentation, enabling uncertainty-aware inference from monocular RGB images. To enable uncertainty-calibrated evidential multi-task learning, we propose a novel evidential depth loss function that jointly optimizes the belief strength of the depth prediction in conjunction with evidential segmentation loss. Building on this, we present EvidKimera, an uncertainty-aware semantic surface mapping framework, which uses evidential depth and semantics prediction for improved 3D metric-semantic consistency. We train and evaluate EvidMTL on the NYUDepthV2 and assess its zero-shot performance on ScanNetV2, demonstrating superior uncertainty estimation compared to conventional approaches while maintaining comparable depth estimation and semantic segmentation. In zero-shot mapping tests on ScanNetV2, EvidKimera outperforms Kimera in semantic surface mapping accuracy and consistency, highlighting the benefits of uncertainty-aware mapping and underscoring its potential for real-world robotic applications.

## I. INTRODUCTION

Semantic scene understanding is a key component in robotic systems, enabling intelligent interaction [1] in applications such as autonomous driving, agriculture, and household robotics. However, for robots to operate reliably in unstructured environments, they should not only recognize objects and surfaces but also quantify the uncertainty in their scene understanding, as wrong predictions over time can lead to inconsistent world models and therefore unreliable decision-making.

For scene understanding and mapping, traditional frameworks initially focused on purely geometric representations [2], [3], which construct spatial occupancy maps but lack semantic context. More recent semantic Truncated Signed Distance Field (TSDF) mapping methods [4], [5] have enabled dense volumetric representations by propagating 2D semantic labels into 3D space [6]. However, these methods often suffer from overconfident predictions, unreliable depth sensing, and ambiguous 2D-to-3D label

All authors are with the Humanoid Robots Lab and the Center for Robotics, University of Bonn, Germany. Nils Dengler and Maren Bennewitz are additionally with the Lamarr Institute, Bonn, Germany.

This work has partially been funded by the Deutsche Forschungsgemeinschaft (DFG, German Research Foundation) under Germany's Excellence Strategy, EXC-2070 – 390732324 – PhenoRob, by the DFG grant 459376902 – AID4Crops, and by the BMBF within the Robotics Institute Germany, grant No. 16ME0999.

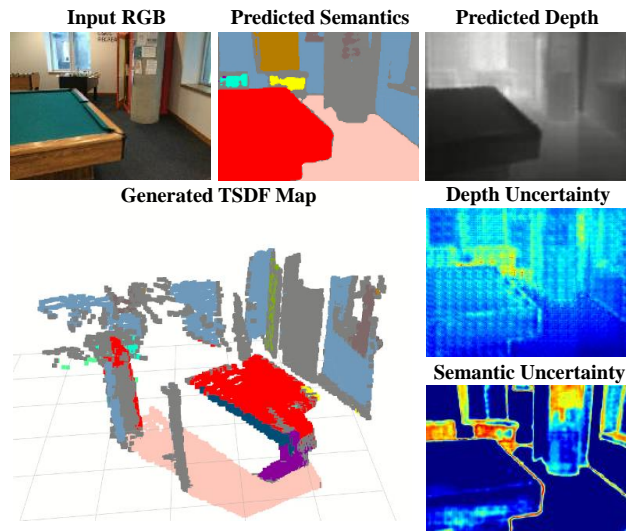


Fig. 1: Visualization of our evidential multi-task perception pipeline. Given RGB data as input, our EvidMTL framework predicts semantic labels and depth along with their corresponding uncertainty estimates. The generated TSDF map from our EvidKimera leverages these uncertainty measurements, only including cells with low depth uncertainty and assigning unknown labels (grey) to regions with high semantics uncertainty.

fusion, leading to inconsistent map representations [7], [8]. This motivates the need for uncertainty-aware methods that quantify confidence in both depth and semantics, allowing robots to make more informed decisions. Hence, semantic and depth predictions have to not only be more accurate but the uncertainties should correlate to the actual errors.

Therefore, Bayesian uncertainty estimation techniques, such as Monte Carlo dropout [9] and ensemble learning [10], have been explored for semantic segmentation but remain computationally expensive due to multiple forward passes or the need for separate network instances [11]. Similarly, while monocular RGB-based depth estimation methods, either standalone [12] or integrated into multi-task frameworks such as SwinMTL [13], help mitigate sparse and noisy depth sensing, they still suffer from overconfidence and unreliability in challenging conditions [14].

To address these limitations, we propose EvidMTL, an evidential multi-task learning framework that extends SwinMTL [13] with uncertainty-aware depth and semantic segmentation. We propose a novel Evidential Scale-Invariant Log (EvidSiLog) loss, which integrates aleatoric uncertainty regularization with a novel prior-anchored Kullback–Leibler (KL) divergence loss. This KL divergence loss optimizes the hyperparameters of evidential depth prediction by anchoring

them to the ground-truth depth prior, ensuring stable and effective joint learning of both tasks. Next, we introduce EvidKimera, a semantic TSDF surface mapping framework that extends the multi-view fusion of Kimera [4] by integrating evidential predictions for depth and semantics. EvidKimera employs a weighting strategy for 2D-to-3D label transfer, discounting unreliable depth estimates to mitigate erroneous updates and incorporating viewpoint similarity to prevent the reinforcement of systematic errors.

To demonstrate the benefits of our loss design, we train and validate our networks on the NYUDepthV2 [15] dataset and justify our approach. Zero-shot testing on ScanNetV2 [16] shows that EvidMTL achieves superior uncertainty estimation compared to conventional approaches while maintaining comparable depth estimation and semantic segmentation performance. To further explore the impact of uncertainty-aware semantic surface mapping, we conduct zero-shot mapping tests on ScanNetV2, confirming that EvidKimera outperforms Kimera in semantic surface mapping accuracy and consistency. The code of our complete pipeline will be made available upon publication.

## II. RELATED WORK

### A. Joint Prediction of Semantic and Depth Information

While dense semantic segmentation is a well-established field of research with convolutional architectures such as U-Net [17], and DeepLab [18], monocular depth estimation methods including Eigen *et al.*'s [19] pioneering work and later works such as Monodepth [20] have investigated learning architectures to predict dense depth maps from monocular RGB images to mitigate noisy and sparse depth sensing. Jointly learning these two modalities not only reduces computational costs but also enhances robustness by leveraging their inter-dependencies.

Recent advancements have shifted towards transformer-based architectures, such as SETR [21] and Swin Transformer [22] for segmentation, and Dense Prediction Transformers (DPT) [23] and AdaBins [24] for depth estimation. These models significantly improve global context modeling but come at the cost of high computational complexity.

Multi-task learning (MTL) has emerged as a promising solution to combine both, leveraging shared representations to improve both semantic segmentation and depth estimation [25]. In this regard, SwinMTL [13] demonstrates how a shared transformer encoder with task-specific output layers can improve accuracy while reducing model size and enhancing computational efficiency.

However, classical deep learning models provide overconfident predictions without quantifying uncertainty, which is critical in safety-sensitive applications like multi-view mapping and autonomous navigation. Bayesian deep learning techniques, such as Monte Carlo dropout [9] and deep ensembles [10], attempt to address this by providing uncertainty estimates. However, their reliance on multiple forward passes significantly increases computational cost, making them impractical for dense prediction tasks.

To overcome these challenges, alternative uncertainty modeling approaches have been proposed, such as evidential classification by Sensoy *et al.* [26] and evidential deep regression by Amini *et al.* [27], which estimate uncertainty without requiring multiple forward passes. While these methods have been explored individually, to the best of our knowledge, no prior work has investigated evidential multi-task learning for jointly predicting semantic segmentation and depth estimation, which we address in this study.

### B. Semantic Mapping

By integrating 3D semantic information derived from 2D images, semantic mapping extends traditional metric maps [2], [3]. Many existing approaches, such as [5], [6] and Kimera Semantics [4], employ Truncated Signed Distance Fields (TSDFs) for dense volumetric mapping. However, they assign semantic labels using majority voting over hard labels from 2D projections, which limits the reliability of the final map.

An alternative approach incorporates raw segmentation logits to represent class probabilities [28]. While this method improves expressiveness, it still suffers from overconfident predictions and lacks a principled way to estimate uncertainty. To mitigate this issue, Bayesian fusion has been explored [29], but it relies on probabilistic neural networks, which introduce significant computational overhead.

The most relevant works to ours are those of Gan *et al.* [30], Kim *et al.* [31] and Marques *et al.* [32], as all four approaches model prior and posterior semantic states using Dirichlet concentration parameters. [30] directly convert one-hot labels from classical segmentation networks into Dirichlet distributions, neglecting measurement uncertainty and thus lacking a true evidential framework. [31] improve upon this by normalizing class probabilities from an evidential segmentation network. However, their method discards individual measurement strength, leading to potential information loss. Both approaches also rely on computationally expensive Bayesian Kernel Inference and infer occupancy states from semantic predictions. While [32] represent 2D semantic states using evidential posteriors, they represent 3D map grid occupancy as binary states in evidential form using the Beta distribution. They do not consider continuous occupancy states nor do they perform evidential depth regression for metric reconstruction. In contrast, our method introduces occupancy-aware evidential fusion, which directly updates semantic posteriors while preserving uncertainty. This ensures a more principled and robust integration of semantic and depth information.

To the best of our knowledge, this is the first work to integrate evidential multi-task learning for uncertainty-aware semantic TSDF mapping from monocular images. Our approach leverages both depth uncertainty-based and viewpoint similarity-based discounting, enhancing fusion quality.

## III. OUR APPROACH

To enable reliable 3D scene reconstruction with uncertainty estimation, we propose evidential multi-task learning

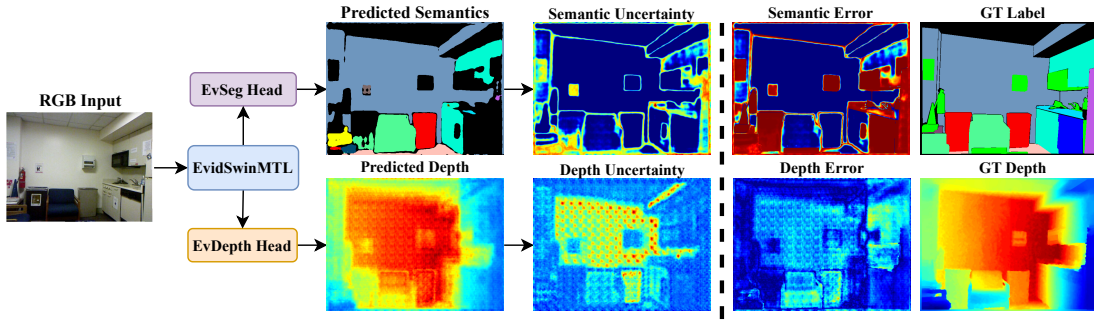


Fig. 2: From an input RGB image our proposed EvidMTL model jointly predicts semantics and depth estimates as well as uncertainty measurements for both. As shown, the uncertainty estimates correspond well to the error in prediction compared to the ground truth (GT).

for depth and semantic predictions from monocular RGB images, along with an uncertainty-aware semantic surface mapping method.

### A. Evidential Multi-Task Learning

For simultaneous semantics and depth prediction, we present **EvidMTL**, an evidential multi-task framework that concurrently predicts semantic labels and depth estimates while explicitly modeling uncertainty, all with a single pass using a shared encoder-decoder architecture, to generate inputs for the proposed mapping approach.

Building upon SwinMTL [13], our framework leverages a Swin Transformer [22] for multi-task learning. This hierarchical vision transformer uses shifted windows to enable efficient self-attention, allowing for joint depth estimation and semantic segmentation. In addition, our framework explicitly models evidential uncertainty for both tasks (semantics and depth) and employs a tailored training scheme that mitigates gradient conflicts caused by the evidential regularization losses. Thus, in contrast to SwinMTL, our approach enables stable multi-task learning and robust, uncertainty-aware predictions for subsequent semantic mapping. Fig. 2 shows that from a single RGB input, our EvidMTL model jointly generates not only semantic segmentation and depth prediction but also their uncertainty estimates. The semantic and depth uncertainty correlate with the semantic and depth error respectively. This enables us to generate calibrated uncertainty-aware semantic maps.

#### 1) Evidential Depth Prediction

To predict the depth observation from RGB input, we assume a Gaussian distribution [33] and model the predicted depth  $\mu$  with a Gaussian prior, placing its conjugate prior, the Normal Inverse Gamma (NIG) distribution, on the variance  $\sigma^2$ . We replace SwinMTL’s depth prediction head with an evidential regression head [27] to generate the evidential depth parameters from the shared decoder. Thus, for each pixel, instead of predicting only the expected depth  $\mu$ , our evidential depth regression head additionally outputs the hyper-parameters of the NIG distribution  $[\alpha, \beta, \nu]$ , where  $\alpha$  quantifies confidence in the expected depth,  $\beta$  captures uncertainty in the depth noise, and  $\nu$  represents the evidence strength or virtual observation counts for  $\mu$ . The expected depth  $\mathbb{E}[d]$ , expected variance  $\mathbb{E}[\sigma^2]$ , and variance in ex-

pected depth  $Var[d]$  are given as follows [27]:

$$\mathbb{E}[d] = \mu, \quad \mathbb{E}[\sigma^2] = \frac{\beta}{\alpha - 1}, \quad Var[d] = \frac{\beta}{\nu(\alpha - 1)} \quad (1)$$

Here,  $\mathbb{E}[\sigma^2]$  represents the aleatoric uncertainty in the depth prediction  $u_{al}^d$ , which is irreducible and attributed to the data, while  $Var[d]$  represents the epistemic uncertainty  $u_{ep}^d$ , which reflects model uncertainty.

We extend the SwinMTL framework by modifying its depth loss to incorporate evidential hyper-parameters. Our novel evidential depth loss  $\mathbb{L}_{ed}$  is defined as:

$$\begin{aligned} \mathbb{L}_{silog} &= \sqrt{\mathbb{E}[(\log d_{gt} - \log \mu)^2] - \lambda \mathbb{E}[\log d_{gt} - \log \mu]^2} \\ \mathbb{L}_{unc} &= \mathbb{E}[\log(1 + \sigma^2)], \quad \mathbb{L}_{reg} = \mathbb{D}_{KL}(\text{NIG}_{pred} \| \text{NIG}_{prior}) \\ \mathbb{L}_{ed} &= \mathbb{L}_{silog} + \lambda_1 \cdot \mathbb{L}_{unc} + \lambda_2 \cdot \min(1.0, (\frac{n_{cur}^{ep}}{k \cdot n_{tot}^{ep}})^2) \cdot \mathbb{L}_{reg} \end{aligned} \quad (2)$$

Here,  $\mathbb{L}_{silog}$  is the Scale-Invariant Log (SiLog) loss [13],  $\mathbb{L}_{unc}$  regularizes predictive uncertainty, and  $\mathbb{L}_{reg}$  is the Kullback–Leibler divergence loss [27] between predicted hyper parameters  $\text{NIG}_{pred}$  and the prior NIG parameters  $\text{NIG}_{prior}$ . Additionally,  $\lambda_1$ ,  $\lambda_2$ , and  $k$  are scaling coefficients,  $n_{cur}^{ep}$  is the current epoch, and  $n_{tot}^{ep}$  is the total number of epochs.

To ensure stable learning, we introduce a square-law annealing for  $\mathbb{L}_{reg}$ , gradually increasing its influence during training. This prevents excessive regularization in early epochs while improving uncertainty-aware depth estimation. Additionally,  $\mathbb{L}_{unc}$  enhances robustness by accounting for predictive uncertainty.

#### 2) Evidential Semantic Segmentation

In order to account for relative class probabilities and uncertainty in predictions, we model semantic segmentation, a multinomial classification task, as a Dirichlet distribution for evidential prediction. Therefore, we extend SwinMTL’s [13] semantic segmentation head with an *evidence layer* that transforms logits into class-specific evidence values using a softplus activation:

$$e_i = \text{softplus}(z_i), \quad c_i = e_i + 1 \quad (3)$$

where  $z_i$  is the logit for class  $i$ , and  $c_i$  parametrizes the Dirichlet distribution. The expected class probabilities and epistemic uncertainty are computed as:

$$S = \sum c_i, \quad p_i = \frac{c_i}{S}, \quad u_{ep}^s = \frac{K}{S} \quad (4)$$

where  $K$  is the number of semantic classes,  $S$  is the total evidence, and  $u_{ep}^s$  represents epistemic uncertainty, derived from Dempster-Shafer theory [34]. The total evidential semantic segmentation loss is defined as:

$$\begin{aligned} \mathbb{L}_{ece} &= \sum_k^K l_k \cdot (\log S - \log c_k) \\ \mathbb{L}_{KL} &= \mathbb{D}_{KL}(Dir(\mathbf{c}) \parallel Dir(\mathbf{1})) \\ \mathbb{L}_{es} &= \mathbb{L}_{ece} + \lambda_3 \cdot \min\left(1.0, \frac{n_{cur}^{ep}}{k \cdot n_{tot}^{ep}}\right) \cdot \mathbb{L}_{KL} \end{aligned} \quad (5)$$

with  $\mathbb{L}_{ece}$  as the evidential cross-entropy loss [26],  $Dir(\mathbf{1})$  the uniform Dirichlet distribution,  $Dir(\mathbf{c})$  the predicted distribution, and  $\mathbb{D}_{KL}$  the Kullback–Leibler divergence.  $\mathbb{L}_{KL}$  acts as a regularizer, mitigating overconfident predictions. This formulation ensures stable multi-task training by dynamically adjusting the strength of the regularization terms. In particular, we apply evidential uncertainty modeling to SwinMTL’s semantic segmentation pipeline and employ linear annealing for semantic regularization to prevent conflicts with the squared-law depth regularization.

### B. Evidential Semantic Surface Mapping

Fig. 3 shows an overview of our proposed architecture and its three components. It comprises three modules: (1) our EvidMTL network predicting depth and semantic segmentation with uncertainty, (2) a cloud creator fusing predictions into an evidential semantic point cloud, and (3) a mapping framework refining the global metric-semantic map via multi-view uncertainty-weighted integration. The individual components are described in the following.

To combine the output of our evidential multi-task network into a meaningful map representation, we propose an uncertainty-aware semantic TSDF mapping framework that integrates an evidential semantic point cloud, formed by fusing the depth and semantic predictions:

$$\mathcal{P} = \left\{ p_i = (\mathbf{x}_i, rgb, u_{ep_i}^d, u_{al_i}^d, c_{i1}, \dots, c_{iK}) \mid i = 1, \dots, N \right\} \quad (6)$$

where  $\mathbf{x}_i = (x_i, y_i, z_i)$  denotes 3D coordinates,  $rgb$  represents color, and  $z_i$  is the expected depth  $\mu$  in the camera frame.

#### 1) Evidential Depth Integration

In comparison to traditional TSDF mapping frameworks such as Voxblox [3] and KinectFusion [35], that assign TSDF weights based on an inverse square law of the depth distance, we propose to incorporate uncertainty-aware weighting. Specifically, we compute the total uncertainty and update the TSDF weights as:

$$u_{tot}^d = u_{ep}^d + u_{al}^d, \quad w_m = \frac{1}{u_{tot}^d}, \quad w_{post} = w_{prior} + w_m \quad (7)$$

where  $u_{tot}^d$  represents the total depth uncertainty,  $w_m$  is the measurement weight, and  $w_{post}$  is the updated weight after incorporating the prior information.

In addition to updating TSDF weights, we also maintain a separate voxel-wise epistemic uncertainty. This uncertainty

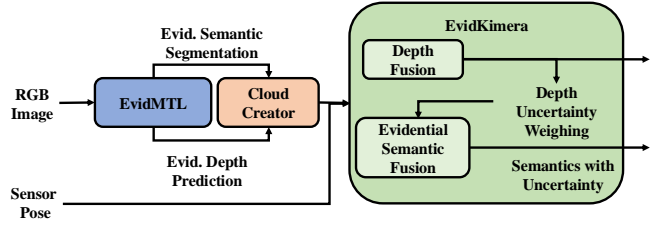


Fig. 3: Our Kimera Semantics Evidential Mapping Framework: The RGB image is processed through an evidential multi-task depth-semantic segmentation network. The resulting semantic point cloud undergoes uncertainty-weighted Bayesian fusion for the TSDF layer, whereas the evidential semantic predictions are used as the measurements for updating the voxel semantic priors. The final uncertainty-weighted fusion refines the semantic voxel posteriors. The mapping framework outputs metric-semantic information with corresponding uncertainties.

is updated in a Bayesian manner, using the harmonic mean of the prior and measurement epistemic uncertainties:

$$\frac{1}{u_{ep}^{post}} = \frac{1}{u_{ep}^{prior}} + \frac{1}{u_{ep}^m} \quad (8)$$

This formulation ensures that the epistemic uncertainty is refined progressively as more observations are incorporated. Unlike conventional TSDF frameworks that solely rely on depth confidence heuristics, our approach explicitly accounts for both aleatoric and epistemic uncertainties, leading to a more robust and uncertainty-aware reconstruction.

#### 2) Evidential Semantic Integration

Typical semantic mapping frameworks use majority voting [36] for hard labels or Bayesian fusion [29] for probabilistic neural networks, often treating the prior, measurement, or posterior as probabilities during fusion. In contrast, we model the semantic state of each voxel entirely within the Dirichlet framework, leveraging its conjugate prior property. This enables a principled fusion process where the prior, measurement, and posterior remain Dirichlet distributions, avoiding conversions between probabilities and distributions [37]. Our approach ensures consistent probabilistic fusion while preserving uncertainty and accumulative evidence.

Beyond the  $K$  semantic classes, we introduce two additional states: free space ( $F$ ) and unknown ( $U$ ), assigned based on TSDF weighting. The semantic state of a voxel is modeled as a Dirichlet distribution  $Dir(\mathbf{c}^{prior})$ , where the concentration parameters include both semantic, free-space and unknown classes, resulting in  $L = K + 2$  total modeled classes. By modeling the background class in the 2D label space differently from the unknown voxel class, we distinguish between confident unknowns and uncertain unknowns.

Given a new measurement  $Dir(\mathbf{c}^m)$ , the posterior update follows:

$$\mathbf{c}^{post} = \mathbf{c}^{prior} + \lambda \mathbf{e}^m, \quad (9)$$

where  $\lambda$  controls the influence of the measurement relative to prior evidence, and  $\mathbf{e}^m = (\mathbf{c}^m - \mathbf{1})$  represents the evidential

belief of the measurement. The class probabilities and hard label assignment are computed as:

$$p_k = \frac{c_k}{S}, \quad S = \sum_{k=1}^L c_k. \quad (10)$$

$$\hat{k} = \begin{cases} \arg \max_k c_k, & \text{if } u_{ep}^s < \tau \\ U, & \text{otherwise.} \end{cases} \quad (11)$$

where  $\tau$  is the uncertainty threshold factor. This formulation ensures a recursive evidential update, maintaining probabilistic structure while accumulating confidence from multiple observations.

### 3) Depth Measurement Weighting

Reliable depth estimates are critical for accurate 2D-to-3D semantic fusion. Instead of assuming uniform confidence, we introduce an *occupancy belief weighting* mechanism that conditions semantic updates on depth uncertainty, ensuring geometric consistency.

**Occupancy belief modeling:** Unlike prior approaches that treat geometric and semantic uncertainties separately, we explicitly incorporate TSDF-based occupancy confidence into semantic updates. The occupancy belief  $o$  is defined as:

$$o = w^m \cdot \begin{cases} 1 - \exp(-|d^m|), & \text{if } d^m > 0 \quad (\text{free space}) \\ \exp(-|d^m|), & \text{if } d^m < 0 \quad (\text{occupied space}) \end{cases} \quad (12)$$

where  $w^m$  is the TSDF weight, and  $d^m$  is the signed distance function (SDF) value. The depth weighting factor  $\lambda_d$  is then computed as:

$$\lambda_d = \max(o, \epsilon) \quad (13)$$

where  $\epsilon = 0.01$ , ensuring that low-confidence measurements contribute minimally.

**Handling free space and unknown regions:** To maintain consistency, semantic updates incorporate depth-aware adjustments:

$$\mathbf{e}^m = \begin{cases} \lambda_d, & d > 0 \quad (\text{free space}) \\ \mathbf{e}^m, & d \leq 0 \quad (\text{occupied space}) \\ \lambda_d, & w < \epsilon \quad (\text{unknown}). \end{cases} \quad (14)$$

By explicitly modeling free-space evidence and preserving uncertainty in unknown regions, this approach ensures robustness to measurement noise while preventing erroneous semantic updates.

### 4) Viewpoint Similarity Discounting

To prevent systematic errors from accumulating, repeated measurements from similar viewpoints are discounted, ensuring that redundant observations do not disproportionately influence the voxel state. Hence, similar to [38], we calculate the viewpoint dissimilarity factor which is used for weighing dissimilar viewpoints over similar ones in semantic measurements.

By integrating these two components into the weighting factor, our framework ensures a robust and uncertainty-aware semantic fusion that maintains consistency across multiple observations while preventing erroneous updates.

## IV. EXPERIMENTAL EVALUATION

The experiments are designed to demonstrate that: (1) The proposed EvidSiLog and  $\text{KL}_\mu$  loss functions in our EvidMTL framework facilitate the generation of calibrated uncertainty estimates. (2) Our EvidMTL network achieves comparable depth and semantic prediction while delivering superior uncertainty estimation compared to a state-of-the-art baseline, particularly on out-of-distribution data. (3) Our evidential mapping framework, EvidKimera, in conjunction with the outputs of our EvidMTL network, produces an accurate and uncertainty-aware semantic map compared to conventional mapping.

### A. EvidMTL Evaluation

#### 1) Metrics and Baseline Methods

To evaluate our proposed EvidMTL model, we evaluate the following metrics for semantic segmentation and depth prediction

- **mIOU:** Semantic segmentation mean Intersection-over-Union.
- **Pixel Acc:** Semantic segmentation pixel accuracy.
- **Seg ECE:** Semantic segmentation expected calibration error, measures the alignment between predicted semantic uncertainty given by Eq. (4), and actual semantic errors.
- **RMSE:** Depth root mean squared error.
- **Depth NLL:** Negative Log-Likelihood, measures how well the predicted depth distribution aligns with the ground truth, penalizing both inaccurate predictions and overconfidence.
- **Depth ECE:** Expected Calibration Error, measures the alignment between predicted depth uncertainty given by Eq. (1) and actual depth errors.
- $\nu$ : Evidence strength in predicted depth.

We train and validate our networks on the NYUDepthV2 dataset [15], which comprises 795 training images and 694 validation images. For out-of-distribution tests, we evaluate the networks on ScanNetV2 [16]. To ensure consistency in semantic labels, we convert the NYU40 labels to the ScanNet20 label space. For a fair comparison, we retrain the baseline method, SwinMTL [13], using a re-implemented version on ScanNet20 classes with the Swin V2 Base SMIM backbone [39], [40].

#### 2) Evaluation Results on NYUDepthV2 Dataset

We conduct an ablation study and comparison to SwinMTL to evaluate the impact of different depth loss formulations within our multi-task learning framework. Specifically, we compare Negative Log-Likelihood (NLL) [27] with our proposed Evidential SiLog loss (Eq. (2)), in combination with evidence regularization (**Reg**), as well as KL divergence without (**KL**) and with (**KL $_\mu$** ) ground truth prior. For KL-based configurations, we set a prior of  $\alpha = 2, \nu = 1, \beta = 0.1$  and apply the prior values as an initialization to Reg-based setups. Additionally, in  $\text{KL}_\mu$ , we use the ground truth depth as the prior for  $\mu$ .

The results of these six ablation configurations are shown in table Tab. I. While NLL serves as the maximum likelihood

Model	mIOU $\uparrow$	Pixel Acc $\uparrow$	Seg. ECE $\downarrow$	RMSE $\downarrow$	Depth NLL $\downarrow$	Depth ECE $\downarrow$	$\nu$
SwinMTL [13]	0.48	<b>0.77</b>	–	<b>0.46</b>	–	–	–
NLL+Reg	0.51	0.76	0.10	3.00	29.05	2.46	$2.0 \times 10^{-3}$
NLL+KL	0.51	0.76	0.08	0.84	4.37	0.52	0.15
NLL+KL $_{\mu}$	0.46	0.74	<b>0.07</b>	0.64	5.67	1.77	*53.7
EvidSiLog+Reg	0.53	0.77	0.08	0.47	1.60	<b>0.31</b>	$1.0 \times 10^{-6}$
EvidSiLog+KL	<b>0.53</b>	0.77	0.08	0.47	1.18	0.83	1.0
EvidSiLog+KL $_{\mu}$ (Our EvidMTL)	0.47	0.76	0.07	0.48	<b>1.01</b>	0.73	*375.09

TABLE I: Semantic and depth performance comparison of the baseline SwinMTL and our proposed network with different losses on NYUDepthV2 validation set. We present six different combinations of depth loss and regularization functions.  $\nu$  represents the evidence strength, indicating whether the depth uncertainty is calibrated. \* indicates the calibrated results, meaning these values are not fixed (no learned confidence) or approaching zero (under confident). As can be seen, (1) EvidSiLog loss outperforms NLL loss, achieving a much lower RMSE. (2) Only the KL $_{\mu}$  loss formulation learns to optimize  $\nu$  based on the ground-truth prior. (3) Our method, EvidMTL (EvidSiLog+KL $_{\mu}$ ), achieves performance comparable to SwinMTL and other alternatives, while also delivering calibrated depth uncertainty.

Model	mIOU $\uparrow$	Pixel Acc $\uparrow$	Seg. ECE $\downarrow$	RMSE $\downarrow$	Depth NLL $\downarrow$	Depth ECE $\downarrow$
SwinMTL [13]	0.35	0.57	–	0.42	–	–
EvidSiLog+Reg	0.35	0.59	<b>0.04</b>	0.43	1.20	0.57
EvidSiLog+KL	<b>0.36</b>	<b>0.60</b>	0.04	<b>0.41</b>	2.48	0.34
EvidSiLog+KL $_{\mu}$ (Our EvidMTL)	0.35	0.58	0.04	0.41	<b>1.10</b>	<b>0.18</b>

TABLE II: Zero-shot semantic and depth results on ScanNetV2 dataset. As can be seen, (1) With EvidSiLog loss, our networks achieve a similar mIOU, Pixel Acc, and RMSE compared to SwinMTL. (2) The KL $_{\mu}$  term facilitates zero-shot generalization of calibrated depth uncertainty, resulting in lower Depth NLL and Depth ECE while maintaining similar Seg. ECE.

estimator for a Gaussian distribution, it performs poorly in our setting, as indicated by its high depth RMSE. We attribute this to gradient imbalance across tasks and the limited training data (795 images versus 25,000 in [27]).

In contrast, EvidSiLog+Reg and EvidSiLog+KL achieve high semantic mIOU and low depth RMSE. However, neither model effectively calibrates depth uncertainty, as their primary loss function does not optimize evidence strength ( $\nu$ ). Finally, although EvidSiLog+KL $_{\mu}$  slightly underperforms in mIOU and RMSE, it successfully calibrates depth uncertainty by leveraging ground truth depth as prior. Note that since the validation set is drawn from the same distribution as the training data, the Depth NLL and Depth ECE metrics show only marginal differences between our calibrated depth uncertainty approach (EvidSiLog+KL $_{\mu}$ ) and the uncalibrated alternatives. However, calibration offers substantial benefits for out-of-distribution depth uncertainty prediction, which we detail in the next subsection.

### 3) Out-of-Distribution Testing on ScanNetV2 Dataset

To assess the zero-shot generalization capability of our model, we evaluate the SwinMTL, EvidSiLog+Reg, EvidSiLog+KL and EvidSiLog+KL $_{\mu}$  models on 10 randomly sampled scenes from the ScanNetV2 [16] dataset’s tasks. Since the models are trained exclusively on the NYUDepthV2 dataset, ScanNetV2 serves as a challenging out-of-distribution (OOD) test set due to domain shifts, despite both datasets containing indoor scenes. The OOD testing results in Tab. II further confirm that: (1) The proposed EvidSiLog loss facilitates effective joint learning of both depth and semantic predictions along with their uncertainties, achieving performance similar to SwinMTL. (2) The proposed KL $_{\mu}$  term calibrates the depth uncertainty, resulting in lower Depth NLL and Depth ECE compared to Reg and KL. To better understand depth uncertainty calibration, we visualize them in Fig. 4. It clearly demonstrates that our

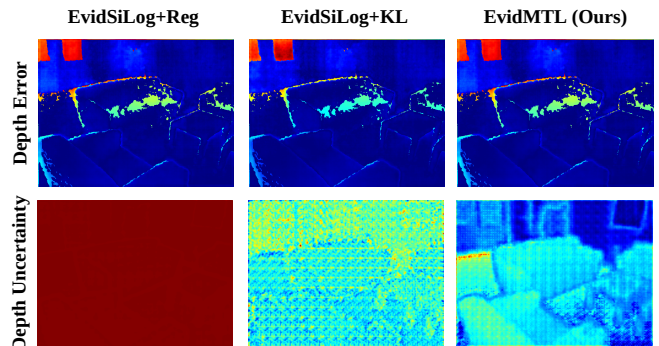


Fig. 4: The top row shows the depth error for a random scene for the zero-shot evaluation of EvidSiLog+Reg, EvidSiLog+KL and EvidMTL on ScanNetV2 dataset. The error and uncertainty increase from blue to red. Due to the extremely low evidence strength  $\nu$ , the EvidSiLog+Reg predicts uniformly high error whereas the EvidSiLog+KL’s uncertainty while slightly better is still not calibrated. Our EvidMTL with the KL $_{\mu}$  improves the predictive depth uncertainty.

EvidMTL yields more visually plausible depth uncertainty predictions.

Although SwinMTL, EvidSiLog+Reg, and EvidSiLog+KL exhibit reasonable zero-shot performance in terms of mIOU, Pixel Acc, and depth RMSE, the errors may remain substantial for downstream tasks such as mapping. In the next section, we explore the importance of introducing uncertainty for the network in the mapping task.

## B. Evidential Semantic Mapping Evaluation

### 1) Metrics and Baseline Methods

To evaluate our evidential semantic mapping framework, we consider multiple metrics to assess the quality of the generated semantic TSDF maps:

- **3D mIOU**: Semantic Mean Cumulative mIOU over all

Model	3D mIOU $\uparrow$	Seg. Voxel Acc $\uparrow$	Seg. Voxel ECE $\downarrow$
Kimera + 2DGT	<b>0.46</b>	<b>0.53</b>	–
Kimera + SwinMTL [13]	0.18	0.29	–
EvidKimera + EvidMTL (Ours)	0.28	0.46	<b>0.44</b>

TABLE III: Zero-shot 3D semantic surface mapping evaluation on the ScanNetV2 dataset. As can be seen, Our EvidKimera + EvidMTL achieves much higher 3D mIOU and Seg. Voxel Acc compared to Kimera + SwinMTL, indicating the benefits of incorporating uncertainty into the framework.

the scenes for voxels in the reconstructed mesh that have a corresponding point in the ground truth mesh within a threshold of the mapping voxel size.

- **Seg. Voxel Acc:** Fraction of voxels that have correct semantic labels.
- **Seg. Voxel ECE:** Similar to 2D ECE, it measures the correlation between the voxel uncertainty and the error in the hard labels.

We consider **EvidKimera + EvidMTL** as our framework, as our EvidKimera framework is only applicable to networks with uncertainty predictions. We compare our approach against **Kimera** [4], which uses TSDFs for dense volumetric mapping and assigns semantics via majority voting on hard labels from 2D projections. For Kimera, we use two different configurations: **Kimera + 2DGT** that uses ground truth depth and ground truth semantic labels as inputs, and **Kimera + SwinMTL** that uses the prediction outputs of SwinMTL. All the three methods use the fast integration mode of Voxblox [3] for pointcloud integration, with a voxel size of 0.04 m. Although we sample all the frames for TSDF layer update, we sample only every fifth frame for semantic layer update for all the methods. For Kimera + 2DGT and Kimera + SwinMTL, we use inverse square law-based depth weighting and majority voting for semantic posterior calculation. For our EvidKimera + EvidMTL, we use the total uncertainty formulation as given in Eq. (7). We randomly sample 5 scenes from the ScanNetV2 dataset [16] for which the ground-truth-labeled meshes were available. To mimic real application scenarios, we perform zero-shot inference without fine-tuning the networks.

## 2) Zero-shot Evaluation Results

As shown in Tab. III, the Kimera + 2DGT establishes an upper bound on the semantic mapping accuracy achieved by conventional mapping pipelines, as it uses ground truth semantic labels and ground truth depth for the surface mapping. Even with 100 percent accuracy in semantic labels, Kimera+ 2DGT is able to achieve only 44 percent cumulative 3D mIOU and 51 percent Seg. Voxel Acc. We postulate that this is due to 2D-to-3D projection errors resulting from inconsistencies in multi-view images, as well as the inherently overconfident nature of hard labels. Kimera + SwinMTL performs considerably worse than our EvidKimera + EvidMTL in terms of 3D mIOU and Seg. Voxel Acc. Although it uses predicted semantics and depth, the absence of uncertainty quantification exacerbates the issue by relying on overconfident yet inaccurate predictions. Unlike the baseline methods, which do not quantify uncertainty, our approach provides voxel-wise uncertainty estimates, enabling more reliable decision-making in ambiguous regions. Note

that while our method has a voxel-wise semantic ECE of 0.44, comparable to state-of-the-art methods that perform 2D semantic calibration fine-tuning [41]. These results confirm that the evidential semantic map representation enables improved uncertainty-aware semantic mapping by taking advantage of the evidential semantic and depth predictions.

## V. CONCLUSION

In this work, we introduce EvidMTL and EvidKimera, which integrate an evidential multi-task learning framework for uncertainty-aware semantic surface mapping from monocular images. Our network, featuring two novel loss terms, jointly predicts semantic segmentation and depth estimation while explicitly modeling uncertainty, thereby enhancing prediction reliability and consistency. Furthermore, we present an evidential semantic mapping framework that leverages uncertainty quantification in both semantic and depth predictions to generate an uncertainty-aware semantic TSDF map. Compared to baselines, our EvidMTL achieves comparable performance in depth and semantic prediction while providing superior uncertainty estimation, particularly in depth uncertainty estimation, which in turn boosts 3D mapping performance in our EvidKimera framework. To our knowledge, this is the first evidential multi-task learning framework for semantic TSDF mapping. Overall, our approach enhances reliability in real-world applications by advancing semantic scene understanding.

## REFERENCES

- [1] S. Garg, N. Sünderhauf, F. Dayoub, D. Morrison, A. Cosgun, G. Carneiro, Q. Wu, T.-J. Chin, I. Reid, S. Gould, *et al.*, “Semantics for robotic mapping, perception and interaction: A survey,” *Foundations and Trends® in Robotics*, 2020.
- [2] A. Hornung, K. M. Wurm, M. Bennewitz, C. Stachniss, and W. Burgard, “Octomap: An efficient probabilistic 3d mapping framework based on octrees,” *Autonomous Robots*, 2013.
- [3] H. Oleynikova, Z. Taylor, M. Fehr, R. Siegwart, and J. Nieto, “Voxblox: Incremental 3d euclidean signed distance fields for on-board mav planning,” in *Proc. of the IEEE/RSJ Intl. Conf. on Intelligent Robots and Systems (IROS)*, 2017.
- [4] A. Rosinol, M. Abate, Y. Chang, and L. Carlone, “Kimera: An open-source library for real-time metric-semantic localization and mapping,” in *Proc. of the IEEE Intl. Conf. on Robotics & Automation (ICRA)*, 2020.
- [5] L. Schmid, J. Delmerico, J. L. Schönberger, J. Nieto, M. Pollefeys, R. Siegwart, and C. Cadena, “Panoptic multi-tdsfs: a flexible representation for online multi-resolution volumetric mapping and long-term dynamic scene consistency,” in *Proc. of the IEEE Intl. Conf. on Robotics & Automation (ICRA)*, 2022.
- [6] M. Grinvald, F. Furrer, T. Novkovic, J. J. Chung, C. Cadena, R. Siegwart, and J. Nieto, “Volumetric instance-aware semantic mapping and 3d object discovery,” *IEEE Robotics and Automation Letters (RA-L)*, 2019.

- [7] C. Guo, G. Pleiss, Y. Sun, and K. Q. Weinberger, "On calibration of modern neural networks," in *Proc. of the Intl. Conf. on Machine Learning*, ser. Proceedings of Machine Learning Research. PMLR, 2017.
- [8] A. Kristiadi, M. Hein, and P. Hennig, "Being bayesian, even just a bit, fixes overconfidence in relu networks," in *Proc. of the Intl. Conf. on Machine Learning*. PMLR, 2020.
- [9] Y. Gal and Z. Ghahramani, "Dropout as a bayesian approximation: Representing model uncertainty in deep learning," in *Proc. of the Intl. Conf. on Machine Learning*. PMLR, 2016.
- [10] B. Lakshminarayanan, A. Pritzel, and C. Blundell, "Simple and scalable predictive uncertainty estimation using deep ensembles," *Advances in Neural Information Processing Systems*, 2017.
- [11] M. Sharma, S. Farquhar, E. Nalisnick, and T. Rainforth, "Do bayesian neural networks need to be fully stochastic?" in *Proc. of the Intl. Conf. on Artificial Intelligence and Statistics (AIS)*. PMLR, 2023.
- [12] Y. Ming, X. Meng, C. Fan, and H. Yu, "Deep learning for monocular depth estimation: A review," *Neurocomputing*, 2021.
- [13] P. Taghavi, R. Langari, and G. Pandey, "SwinMTL: A shared architecture for simultaneous depth estimation and semantic segmentation from monocular camera images," in *Proc. of the IEEE/RSJ Intl. Conf. on Intelligent Robots and Systems (IROS)*, 2024.
- [14] S. Gasperini, N. Morbitzer, H. Jung, N. Navab, and F. Tombari, "Robust monocular depth estimation under challenging conditions," in *Proc. of the IEEE/CVF Conf. on Computer Vision and Pattern Recognition (CVPR)*, 2023.
- [15] P. K. Nathan Silberman, Derek Hoiem and R. Fergus, "Indoor segmentation and support inference from rgbd images," in *Proc. of the Europ. Conf. on Computer Vision (ECCV)*, 2012.
- [16] A. Dai, M. Nießner, M. Zollöfer, S. Izadi, and C. Theobalt, "Bundlefusion: Real-time globally consistent 3d reconstruction using on-the-fly surface re-integration," *ACM Transactions on Graphics (TOG)*, 2017.
- [17] O. Ronneberger, P. Fischer, and T. Brox, "U-net: Convolutional networks for biomedical image segmentation," in *Medical image computing and computer-assisted intervention—MICCAI 2015: 18th international conference*. Springer, 2015.
- [18] C. Liang-Chieh, G. Papandreou, I. Kokkinos, K. Murphy, and A. Yuille, "Semantic image segmentation with deep convolutional nets and fully connected crfs," in *Proc. of the Intl. Conf. on Learning Representations*, 2015.
- [19] D. Eigen, C. Puhrsch, and R. Fergus, "Depth map prediction from a single image using a multi-scale deep network," *Advances in Neural Information Processing Systems*, 2014.
- [20] C. Godard, O. Mac Aodha, and G. J. Brostow, "Unsupervised monocular depth estimation with left-right consistency," in *Proc. of the IEEE/CVF Conf. on Computer Vision and Pattern Recognition (CVPR)*, 2017.
- [21] S. Zheng, J. Lu, H. Zhao, X. Zhu, Z. Luo, Y. Wang, Y. Fu, J. Feng, T. Xiang, P. H. Torr, *et al.*, "Rethinking semantic segmentation from a sequence-to-sequence perspective with transformers," in *Proc. of the IEEE/CVF Conf. on Computer Vision and Pattern Recognition (CVPR)*, 2021.
- [22] Z. Liu, H. Hu, Y. Lin, Z. Yao, Z. Xie, Y. Wei, J. Ning, Y. Cao, Z. Zhang, L. Dong, *et al.*, "Swin transformer v2: Scaling up capacity and resolution," in *Proc. of the IEEE/CVF Conf. on Computer Vision and Pattern Recognition (CVPR)*, 2022.
- [23] R. Ranftl, A. Bochkovskiy, and V. Koltun, "Vision transformers for dense prediction," in *Proc. of the IEEE Intl. Conf. on Computer Vision (ICCV)*, 2021.
- [24] S. F. Bhat, I. Alhashim, and P. Wonka, "Adabins: Depth estimation using adaptive bins," in *Proc. of the IEEE/CVF Conf. on Computer Vision and Pattern Recognition (CVPR)*, 2021.
- [25] S. Vandenhende, S. Georgoulis, W. Van Gansbeke, M. Proesmans, D. Dai, and L. Van Gool, "Multi-task learning for dense prediction tasks: A survey," *IEEE Trans. on Pattern Analysis and Machine Intelligence (TPAMI)*, 2021.
- [26] M. Sensoy, L. Kaplan, and M. Kandemir, "Evidential deep learning to quantify classification uncertainty," *Advances in Neural Information Processing Systems*, 2018.
- [27] A. Amini, W. Schwarting, A. Soleimany, and D. Rus, "Deep evidential regression," *Advances in Neural Information Processing Systems*, 2020.
- [28] N. Sünderhauf, T. T. Pham, Y. Latif, M. Milford, and I. Reid, "Meaningful maps with object-oriented semantic mapping," in *Proc. of the IEEE/RSJ Intl. Conf. on Intelligent Robots and Systems (IROS)*, 2017.
- [29] D. Morilla-Cabello, L. Mur-Labadia, R. Martinez-Cantin, and E. Montijano, "Robust fusion for bayesian semantic mapping," in *Proc. of the IEEE/RSJ Intl. Conf. on Intelligent Robots and Systems (IROS)*, 2023.
- [30] L. Gan, R. Zhang, J. W. Grizzle, R. M. Eustice, and M. Ghaffari, "Bayesian spatial kernel smoothing for scalable dense semantic mapping," *IEEE Robotics and Automation Letters (RA-L)*, 2020.
- [31] J. Kim, J. Seo, and J. Min, "Evidential semantic mapping in off-road environments with uncertainty-aware bayesian kernel inference," in *Proc. of the IEEE/RSJ Intl. Conf. on Intelligent Robots and Systems (IROS)*, 2024.
- [32] J. M. C. Marques, N. Dengler, T. Zaenker, J. Mucke, S. Wang, M. Bennewitz, and K. Hauser, "Map space belief prediction for manipulation-enhanced mapping," 2025.
- [33] A. Belhedi, A. Bartoli, S. Bourgeois, V. Gay-Bellile, K. Hamrouni, and P. Sayd, "Noise modelling in time-of-flight sensors with application to depth noise removal and uncertainty estimation in three-dimensional measurement," *IET Computer Vision*, 2015.
- [34] G. Shafer, "Dempster-shafer theory," *Encyclopedia of artificial intelligence*, 1992.
- [35] R. A. Newcombe, S. Izadi, O. Hilliges, D. Molyneaux, D. Kim, A. J. Davison, P. Kohi, J. Shotton, S. Hodges, and A. Fitzgibbon, "Kinectfusion: Real-time dense surface mapping and tracking," in *2011 10th IEEE international symposium on mixed and augmented reality*. IEEE, 2011.
- [36] Z. Zhao and X. Chen, "Semantic mapping for object category and structural class," in *Proc. of the IEEE/RSJ Intl. Conf. on Intelligent Robots and Systems (IROS)*, 2014.
- [37] B. A. Frigyik, A. Kapila, and M. R. Gupta, "Introduction to the dirichlet distribution and related processes," *Department of Electrical Engineering, University of Washington, UWEETR-2010-0006*, 2010.
- [38] R. Menon, T. Zaenker, N. Dengler, and M. Bennewitz, "Nbv-sc: Next best view planning based on shape completion for fruit mapping and reconstruction," in *Proc. of the IEEE/RSJ Intl. Conf. on Intelligent Robots and Systems (IROS)*, 2023.
- [39] Z. Xie, Z. Geng, J. Hu, Z. Zhang, H. Hu, and Y. Cao, "Revealing the dark secrets of masked image modeling," in *Proc. of the IEEE/CVF Conf. on Computer Vision and Pattern Recognition (CVPR)*, 2023.
- [40] D. Kim, W. Ka, P. Ahn, D. Joo, S. Chun, and J. Kim, "Global-local path networks for monocular depth estimation with vertical cutdepth," arXiv preprint arXiv:2201.07436.
- [41] J. M. C. Marques, A. J. Zhai, S. Wang, and K. Hauser, "On the overconfidence problem in semantic 3d mapping," in *Proc. of the IEEE Intl. Conf. on Robotics & Automation (ICRA)*, 2024.